Magnetic Basement:
Gravity-Guided Magnetic Source Depth Analysis and Interpretation

Serguei A. Goussev, Fugro Robertson Inc., Houston, U.S.A.,
John W. Peirce, GEDCO, Calgary, Canada

Summary

We present an integrated approach to the interpretation of magnetic basement that is based on recognition of characteristic patterns in distributions and alignments of magnetic source depth solutions above and below the surface of magnetic basement. This approach integrates a quantitative analysis of depth solutions, obtained by 2D Werner deconvolution and 2D Euler deconvolution of the magnetic data, with a qualitative evaluation of the Bouguer gravity anomalies. The crystalline/metamorphic basement and sedimentary cover have different origins, tectonic histories, lithologies and characteristics of magnetization. These differences result in different geometries of magnetic sources associated with faults, fracture zones, igneous intrusions, erosional truncations, subcrop edges and other structural discontinuities. Properly tuned, the automated depth-to-source estimation techniques, like 2D Werner deconvolution and 2D Euler deconvolution, are often capable of resolving the intra-sedimentary and intra-basement magnetic source geometries into distinctly different distributions and alignments of clustered depth solutions. An empirical set of criteria, "basement indicators", was developed for identification and correlation of the basement surface. The ambiguity of basement correlation with a limited or non-available well control, which is typical for onshore frontier and offshore explorations, can be reduced by incorporating the Bouguer gravity data into the process of correlation.

Introduction

There are two main approaches to the mapping of magnetic basement using the magnetic and/or gravity data: depth-to-magnetic source analysis and 3D modeling with subsequent structural inversion.

Basement mapping with the depth-to-magnetic source techniques has been in use for several decades. The working concept is that dominant anomalies in the observed magnetic field are generated by sources near the basement top (Nabighian et al., 2005). There are several proven techniques, both manual and automated, that provide calculations of the magnetic source depth solutions (Li, 2003). Different methods work best for different simplified source geometries like thin dike, contact, sphere, horizontal or vertical cylinder, etc. Manual/graphical methods relate the magnetic source depth to measured distances between characteristic points of the anomaly's profile. The automated methods, like 2D Werner deconvolution and 2D Euler deconvolution, work on profiles of magnetic data. Their algorithms, using simplified source geometry approximations and different calculation parameters (structural index or else), solve a system of redundant equations for magnetic source parameters, including location and depth. The

complicating factors are anomalies' interference, noise contamination, igneous intrusions penetrating deeply into the sedimentary section and, often, sparse distribution of "reliable" depth solutions that make accuracy and lateral resolution of the basement interpretation below expectations of the modern oil and gas exploration in structurally complex areas.

3D modeling and structural inversion are based on construction of 3D magnetic or gravity model of subsurface from available data that is inverted for the basement depth (Nabighian et al., 2005). The working concept is that the model misfit (i.e. difference between the observed magnetic or gravity field and that of calculated from the constructed 3D model) can be assigned to unknown variations of the basement depth and, hence, inverted for it. The accuracy and lateral resolution of 3D structural inversion are strongly dependent on information about magnetic susceptibility and density of basement rocks and the initial basement structure chosen. Such information is, usually, very limited or not available.

In mid-90s, one of us (JWP) proposed a new approach to the magnetic basement mapping from the High-Resolution AeroMagnetic (HRAM) data that was implemented and used extensively, mostly in the Western Canada Sedimentary Basin. This approach is based on experience of analysis of distributions and alignments of magnetic depth solutions, obtained by automated depth-to-source techniques, near wells that penetrated the crystalline/metamorphic basement. An empirical set of 'basement indicators" was developed for identification and correlation of the basement surface using available well control. However, in onshore frontier areas and offshore/marine exploration, the basement penetrating wells are rare or not available. This lack of well control can be, in part, compensated by integration with the Bouguer gravity data. Usually, the gravity data are acquired in marine acquisition concurrently with the magnetic data or available from the airborne or ground acquisition in onshore frontier areas.

Methodology

There are three definitions of the basement used in the exploration: geologic, magnetic and acoustic. Often these terms are used loosely and interchangeably although they have distinctly different meanings.

By definition of the "Glossary of Geology" by the American Geological Institute (Neuendorf et al., 2005), the geologic basement is "the crust of the Earth below sedimentary deposits, extending downward to the Mohorovicic discontinuity. In many places the rocks of the complex are igneous and metamorphic and of Precambrian age, but in some places they are Paleozoic, Mesozoic or even Cenozoic." (p.57). The magnetic basement is "the upper surface of extensive heterogeneous rocks having relatively large magnetic susceptibilities compared with those of sediments; often but not necessarily coincident with the geologic basement" (p.389).

By definition of the "Encyclopedic Dictionary of Applied Geophysics" (Sheriff, 2006, p.2), the acoustic basement is "the deepest more-or-less continuous seismic reflector;

often an unconformity below which seismic energy returns are poor or absent. Also called seismic basement."

For the purposes of our approach, it should be noted that a) geologic basement and magnetic basement can be the same geological boundary; b) acoustic basement, which is often used as an upper constraint for the magnetic basement interpretation, can be structurally close or locally coincident with the geologic/magnetic basement.

The difference between our approach and traditional interpretation of magnetic basement with automated depth-to-source estimation methods is four-fold. First, it is based on the use of multiple variable width moving widows to obtain many more depth solutions than usual, and to cover a wide range of depths around the expected basement level. Calculations with multi-width windows can enhance the appearance of depth solution associated with real magnetic sources by "stacking" obtained solutions in a way similar to the multi-offset seismic Common Depth Point (CDP) technique in order to differentiate "real" magnetic source depth solutions from numerous "noise" depth solutions. Second, our approach takes into consideration not only solutions, assumed to be associated with the basement top, but also those within the sedimentary section, i.e. distributions and alignments of obtained depth solutions above and below the basement surface are considered. Third, we integrate the Bouguer gravity as independent source of structural data into a process of the basement horizon correlation. Fourth, the basement is mapped as a line-by-line correlated continuous horizon, not as isolated depth picks, with additional depth control and ties of correlation at line intersections.

From several automated depth-to-source estimation techniques, proven to be reliable and efficient in application for the last 15-20 years, we use 2D Werner deconvolution and 2D Euler deconvolution for the line-by-line magnetic source depth calculations. Manual/graphic methods (straight-slope, half-slope, Bean-ratio-A and others) are also used for depth estimates at locations where magnetic anomalies seem to be undisturbed by interference.

The working concept of our approach is based on five corroborating types of evidence, generally defined as geological, magnetic, modeling, gravity and empirical evidence.

Lateral heterogeneity of magnetization is a necessary pre-condition for the presence of magnetic anomalies. The magnetic anomaly of exploration interest can be defined as a response of the magnetic field to the lateral change in magnetic susceptibility contrast. If there is no change, then there is no anomaly. And every magnetic anomaly, for the purposes of automated calculations of its source's depth, can be approximated with simplified source geometry.

The "geological" evidence comes from recognition of differences between the metamorphic/magnetic basement and sedimentary cover in their origins, tectonic histories, lithologies and characteristics of magnetization. These differences result in different patterns of lateral magnetic heterogeneity associated with faults, fracture zones, porosity, igneous intrusions, erosional truncations, subcrop edges and other structural

discontinuities. Among other contributors to these differences are the hydrothermal fluids, also called "juvenile water" ("Glossary of Geology", p. 346), produced in large quantities by the process of magma transition from the liquid state into the solid one. We hypothesize that their abnormally high pressure and temperature push these fluids into the sedimentary section to open and fill-in faulted, fractured and porous sedimentary rocks to enter into chemical reactions and precipitate magnetic minerals, i.e. act in a way similar to "barium meal" for the X-ray examination. All together, the differences in lateral magnetic heterogeneity make a basis for the presence of different magnetic source geometries in the basement and sedimentary cover.

The "magnetic" evidence comes from relatively recent discoveries of new types of magnetic anomalies generated by sources within the sedimentary section. The release of the Global Positioning System (GPS) into commercial application provided for magnetic acquisition along closely spaced lines and getting grids with short-wavelength anomalies undetectable with wide line spacing. Advances in data processing made possible separation of short- and mid-wavelength intra-sedimentary anomalies from interference with both near-surface noise and deep intra-basement anomalies. From a long list of publications related to the intra-sedimentary sources and anomalies, we refer the reader to several papers: intra-sedimentary igneous intrusions (Brown et al., 1994; Kjarsgaard et al., 1994); secondary magnetization along fault zones (Gunn, 1997; Peirce et al., 1998); juxtaposition of layers with differing magnetization (Grauch et al., 2001 and 2006); continuous magnetic horizons (Abaco and Lawton, 2003); magnetic formations offset by faults (Grauch et al., 2001; Goussev et al., 2003), and intra-sedimentary magnetic source depth solutions associated with subsurface erosional truncations and faults (Peirce et al., 1998; Goussev et al., 1998; Glenn et al., 2002). The "magnetic" evidence proves the existence of a) intra-sedimentary sources and detectable intra-sedimentary anomalies and b) intra-sedimentary magnetic source depth solutions that can be obtained as distributions and alignments separate from the basement ones.

The "modeling" evidence is illustrated by results of 2D magnetic modeling and simulation of the magnetic source depth solutions, published in a "Round Table" discussion Peirce et al. and Pawlowski (1999) in the The Leading Edge. Jain (1976) shows that multiple runs of automated calculations of Werner 2D depth solutions with variable size sliding windows for uniformly magnetized vertical dike result in a vertical dispersion of the magnetic depth solutions or, in other words, an artificial "tail" aligned vertically downward from dike's top. The authors in the "Round Table" discussion reproduced these "tails" of uniformly magnetized homogeneous dikes and, in addition, modeled three non-uniformly magnetized heterogeneous dikes with their susceptibilities and widths increasing with depth (i.e. geologically plausible approximation of a magnetized fault or fracture zone). With standard clustering parameters, the depth solutions are dispersed along the entire depth extent of dikes (Figure 1, upper panel). With tight clustering parameters, the vertical dispersion is reduced to about half of the extent of the center dike and about ¾ of the extent of two other dikes (Figure 1, middle panel). The conclusion was that a) both uniformly and non-uniformly magnetized dikes produced vertical alignments ("tails") of clustered depth solutions of various extent and b) alignments are sensitive to magnetic properties, source shape and clustering

parameters, i.e. vertical heterogeneity in magnetization can result in a longer alignment of solutions enhanced by both dispersion of artificial solutions, due to variable window width, and "real" depth solutions associated with magnetic heterogeneity. Apparently, neither Werner deconvolution nor Euler deconvolution can resolve all heterogeneous parts of dikes, but the heterogeneity itself seems to be instrumental in producing additional solutions to enhance the alignments associated with three heterogeneous dikes. The "modeling" evidence is important for our application as it shows that a visible presence of depth solutions, associated with real magnetic sources, can be enhanced using multi-width sliding windows and proper selection of clustering parameters as compared to randomly distributed noise solutions, generated by the calculation algorithms in the absence of real sources.

The "gravity" evidence comes from a proven fact that every large basement structure, structural high or structural low, has its corresponding Bouguer gravity anomaly. Obviously, the opposite is not necessarily true: not every Bouguer gravity anomaly is associated with the basement structure. Salt tectonics, shale diapirism, thin-skin thrusting and other elements of the sedimentary structure generate anomalies that can dominate the Bouguer gravity field. Accordingly, our integrated approach does not just mimic the Bouguer gravity anomalies. With a proper discretion, we evaluate and incorporate them into the process of basement correlation as a source of independent structural information to be used as a guide for making a choice between two alternative correlations: up or down along the interpreted line.

The "empirical" evidence is based on the experience of analysis of distributions and alignments of the magnetic source depth solutions near wells that penetrated the crystalline/metamorphic basement. Putting aside arguments about the nature of obtained alignments or "tails" of depth solutions, we believe that for the purposes of basement correlation it does not matter what any specific alignment or "tail" represents: actual distribution of magnetic sources along a heterogeneously magnetized fault/fracture zone or merely a dispersion of artifacts produced by calculations with windows of different widths. What matters is that real magnetic sources and their assemblages, as 2D modeling shows, always have regular "tails" while noise depth solutions are much more random in their distributions and, often, have no "tails". In practice of the basement horizon correlation, it is a powerful criterion that helps to reduce the inherent ambiguity of discrimination between real magnetic source depth solutions and numerous noise depth solutions.

The following empirical set of "basement indicators" was developed (Figure 2): 1) "lateral alignment" – depth solutions align laterally along the basement surface; 2) "truncation"- vertical or near-vertical alignments of intra-sedimentary and intra-basement depth solutions truncate along the basement surface; 3) "change of dip"- alignments of depth solutions abruptly change their apparent dip, sometimes, to the opposite direction across the basement surface; 4) "gap" – zone without depth solutions between clusters of intra-sedimentary and intra-basement solutions; 5) "alignment into cloud"- intra-basement vertical alignment of depth solutions transforms into a cloud of solutions across

the basement surface; 6) “bounded noise” – laterally extended cloud of noise solutions is bounded from below or above by the basement surface.

The line-by-line correlation of the basement horizon with “basement indicators” is much less ambiguous than basement mapping with traditional methods, but it is still an interpretive process, especially in areas without well control. Placing profiles of the Bouguer gravity immediately above cross-sections with magnetic source depth solutions, with a proper discretion applied, will guide the correlation in the right direction: up or down laterally along the interpreted line. Additional “decision-making” information can be obtained when enhanced gravity and magnetic grids are simultaneously displayed on a dual-screen workstation.

The important feature of the described approach is that the “basement indicators” can be applied not only to the crystalline/metamorphic basement, but, sometimes, to the regional unconformities like pre-rift basement in the continental margins where this basement is not necessarily crystalline/metamorphic and highly magnetic.

Interpretation Examples

Figure 3 shows three examples of the MagProbe^{TM} depth cross-sections overlain with the acoustic basement horizon (magenta). There are five basement indicators here: “gap” and “bounded noise” (a), “change of dip” (b), “truncation” and “lateral alignment” (c). Subtle but consistent in appearance, these basement indicators are recognizable at the background of noise depth solutions attenuated by tight clustering. On these examples, the acoustic basement is coincident with the interpreted magnetic basement.

Figure 4 shows examples of five basement indicators (red ellipses): one “truncation” in the left part of the cross-section and three “truncations” and “bounded noise” in the right part, where the basement uplift is formed by a prominent igneous body. On this line, the acoustic basement is about 1.5 km shallower (on the right) and about 0.5 km deeper (on the left) than the interpreted magnetic basement.

Figure 5 shows the basement indicators on a cross-section from the Peace River Arch in Alberta, Canada (Rhodes and Peirce, 1999), overlain with two interpreted horizons, Precambrian basement and Mesozoic unconformity, and five basement penetrating wells. Note that in this example basement indicators are also applicable to the Mesozoic unconformity because the sediments in this area are relatively high in iron content.

Figures 6 and 7 show examples of basement horizon correlation on the MagProbe^{TM} cross-sections integrated with the Bouguer gravity profiles. Figure 6 shows that without the acoustic basement control, the magnetic basement structural high can be missed to alternative interpretation (yellow horizon) of basement indicators and the Bouguer gravity profile “guides” the correlation of the basement horizon in the right direction. Figure 7 shows the interpretation example where the basement horizon (blue) could be, most probably, correlated as a structural high (alternative correlation in green) while the

long-wavelength component of the Bouguer gravity profile clearly shows the presence of an opposite structure, i.e. structural low.

Conclusions

1. Magnetic basement and sedimentary cover have recognizable differences in magnetic source geometries as represented by distributions and alignments of depth solutions, obtained by application of 2D Werner deconvolution and 2D Euler deconvolution techniques.
2. The empirical set of criteria, “basement indicators” has been developed for identification and correlation of the magnetic basement horizon.
3. Integration with the Bouguer gravity provides much less ambiguous basement correlation where well control is limited or non-available.

This presented approach is a logical step in further development of traditional methods that moves the magnetic basement interpretation to a higher level of confidence. As any interpretation method, this approach has its limitations and subject to complications, like interference of anomalies and noise contamination that pose difficulties in structurally complex areas of the oil and gas exploration.

The advantages of this approach, as compared to other methods, are 1) enhanced visualization of depth solutions associated with real magnetic sources; 2) higher lateral resolution of the magnetic basement structure as not only intra-basement depth solutions, but also intra-sedimentary ones are taken into consideration; 3) line-by-line correlation of the basement horizon with elimination of mis-ties at line intersections adds to higher accuracy of the basement depth interpretation; 4) integration with the Bouguer gravity, as independent source of structural information, helps to reduce the ambiguity of basement horizon correlation; 5) empirical “basement indicators”, that we use for identification of the basement surface, have been tested and proven by several years of interpretation under various geological environments.

Acknowledgements

We would like to acknowledge Fugro Robertson Inc. (FRI) and GEDCO for permission to publish this paper, Mark Weber, FRI President, and Rao Yalamanchili, VP Interpretation, for critical comments and suggestions that helped to improve this paper, Vsevolod Egorov of FRI for technical assistance and two oil companies, that preferred to stay anonymous, for permission to use their data.

References

1. Abaco, C.I., and Lawton, D.C., 2003. Magnetic anomalies in the Alberta foothills, Canada. *SEG Expanded Abstracts* **22**, 612-615.
2. Brown, G., Platt, N.H., and McGrandle, A., 1994. The geophysical expression of Tertiary dikes in the southern North Sea. *First Break* **12**,137-146.
3. Glenn, W.E., Rhodes, J.A., Goussev, S.A., Benedict, M.N., Charters, R.A., and Peirce, J.W., 2002. Aeromagnetic depth solutions indicate numerous magnetic sources within the sedimentary section in the Western Canada Sedimentary Basin. *CSEG Expanded Abstracts*, 132-134.
4. Goussev, S.A., Charters, R.A., Peirce, J.W., and Glenn, W.E., 2003, Jackpine Creek magnetic anomaly: Identification of a buried meteorite impact structure. *The Leading Edge* **22**, 740-741.
5. Goussev, S.A., Charters, R.A., Hassan, H.H., Peirce, J.W., and Genereux, J., 1998. HRAM fault interpretation using MagProbe^{TM} depth estimates and non-traditional filtering. *Canadian Journal of Exploration Geophysics* **34**, 30-39.
6. Grauch, V.J.S., Hudson, M.R., Minor, S.A., and Caine, J.S., 2006. Sources of along-strike variation in magnetic anomalies related to intra-sedimentary faults: A case study from the Rio-Grande Rift, USA. *AESC*, Melbourne.
7. Grauch, V.J.S., Hudson, M.R., and Minor, S.A., 2001. Aeromagnetic expression of faults that offset basin fill, Albuquerque basin, New Mexico. *Geophysics* **66**, 707-720.
8. Gunn, P.J., 1997. Application of aeromagnetic surveys to sedimentary basin studies. *AGSO Journal of Australian Geology and Geophysics* **17**, 133-144.
9. Jain, S., 1976. An automated method of direct interpretation of magnetic profiles. *Geophysics* **41**, 531-545.
10. Kjarsgaard, B.A., and Davis, W.J., 1994. Eocene Magmatism, Sweet Grass Hills: Expression and Significance. *Lithoprobe Report* **37**, 234-237.
11. Li, X., 2003. On the use of different methods for estimating magnetic depth. *The Leading Edge* **22**, 1090-1099.
12. Nabighian, M.N., Grauch, V.J.S., Hansen, R.O., LaFehr, T.R., Li, Y., Peirce, J.W., Phillips, J.D., and Ruder, M.E., 2005. The historical development of the magnetic method in exploration. *Geophysics* **70**, 33ND-61ND.
13. Neuendorf, K.K.E., Mehl, J.P., and Jackson, J.A. (eds), 2005. *Glossary of Geology*, 5th edition. American Geological Institute. ISSN 0300-7227.
14. Peirce, J.W., Goussev, S.A., Charters, R.A., Abercrombie, H.J., and DePaoli, G.R., 1998. Intra-sedimentary magnetization by vertical fluid flow and exotic geochemistry. *The Leading Edge* **17**, 89-92.
15. Peirce, J.W., Goussev, S.A., Charters, R.A., Abercrombie, H.J., and DePaoli, G.R., and Pawlowski, R., 1999. Round Table discussion. *The Leading Edge* **18**, 211-214.
16. Rhodes, J.A, and Peirce, J.W., 1999. MaFIC-Magnetic Interpretation in 3D using a seismic workstation. *SEG Expanded Abstracts* **18**, 335-338.
17. Sheriff, R.E., 2006. *Encyclopedic Dictionary of Applied Geophysics*, 4th edition, Society of Exploration Geophysics. ISBN 1-56080-118-2.

Figure Captions:

Figure 1. Model simulation of clustered magnetic source depth solutions (modified from Peirce et al., 1999).
Upper panel: Werner deconvolution (red) and Euler deconvolution (green) depth solutions obtained using a small cluster.
Middle panel: Werner deconvolution (red) and Euler deconvolution (green) depth solutions obtained using a big cluster.
Lower panel: model cross-sections with homogeneous dikes (left) and heterogeneous dikes (right);

Figure 2. Empirical basement indicators: 1-“lateral alignment”; 2-“truncation”; 3-“change of dip”; 4-“gap”; 5-“alignment into cloud”; 6-“bounded noise”.

Figure 3. Examples of basement indicators in real data: “gap” and “bounded noise” (left), “change of dip” (center), “truncation” and “lateral alignment” (right). Acoustic basement horizon is shown in magenta.

Figure 4. Basement horizon correlation using basement indicators (red ellipses): “truncation” on the left and three “truncations” and “bounded noise” on the right. Acoustic basement horizon is shown in magenta and correlated magnetic basement horizon in yellow.

Figure 5. Basement horizon correlation (red) on the MaFIC cross-section overlain with Mesozoic Unconformity horizon from wells (brown) and five Precambrian wells (“W”).

Figure 6. Examples of basement indicators (red ellipses) on the MagProbe^{TM} cross-section overlain with acoustic basement horizon (magenta). Alternative correlation is shown in yellow. Bouguer gravity profile (red) and its horizontal derivative (green) are shown in the upper part.

Figure 7. Basement horizon correlation on the MagProbe^{TM} cross-section with the Bouguer gravity profile. Basement horizon is shown in dark blue with diagonal crosses and alternative correlation is shown in green. Bouguer gravity profile (light blue) is in the upper part.

Figure 1.

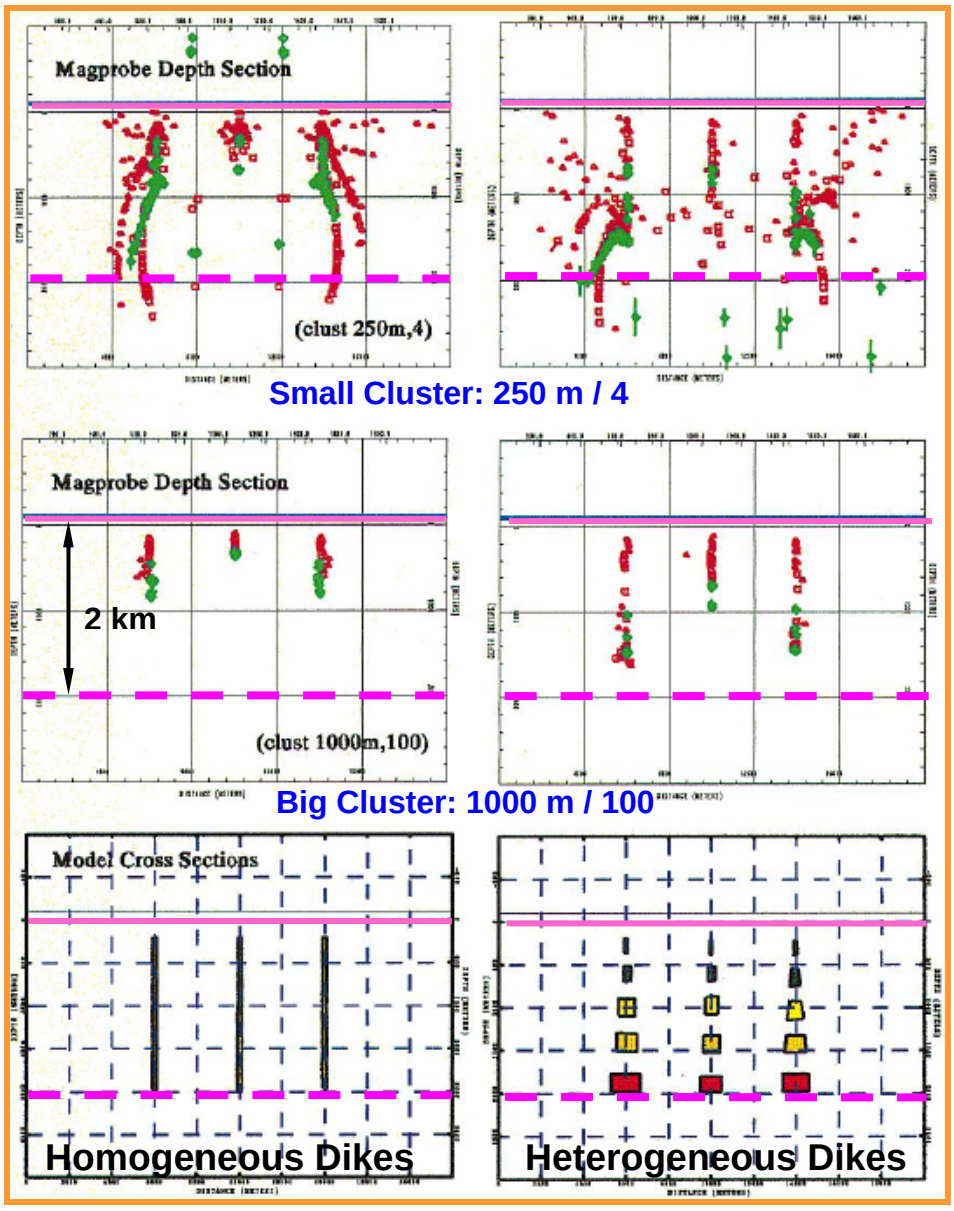
Magprobe Depth Section
(clust 250m,4)
Small Cluster: 250 m / 4
Magprobe Depth Section
2 km
(clust 1000m,100)
Big Cluster: 1000 m / 100
Model Cross Sections
Homogeneous Dikes
Heterogeneous Dikes

Figure 2.

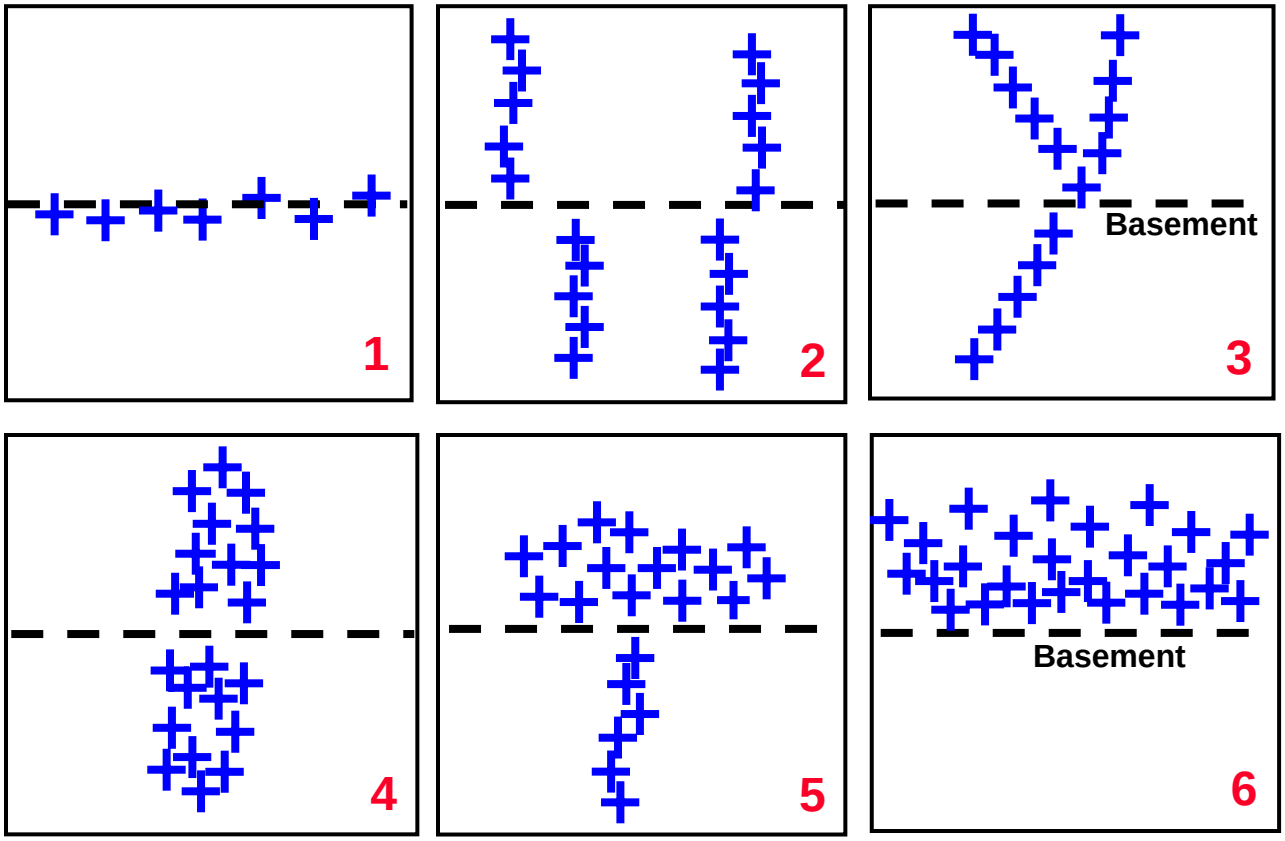

Figure 3.

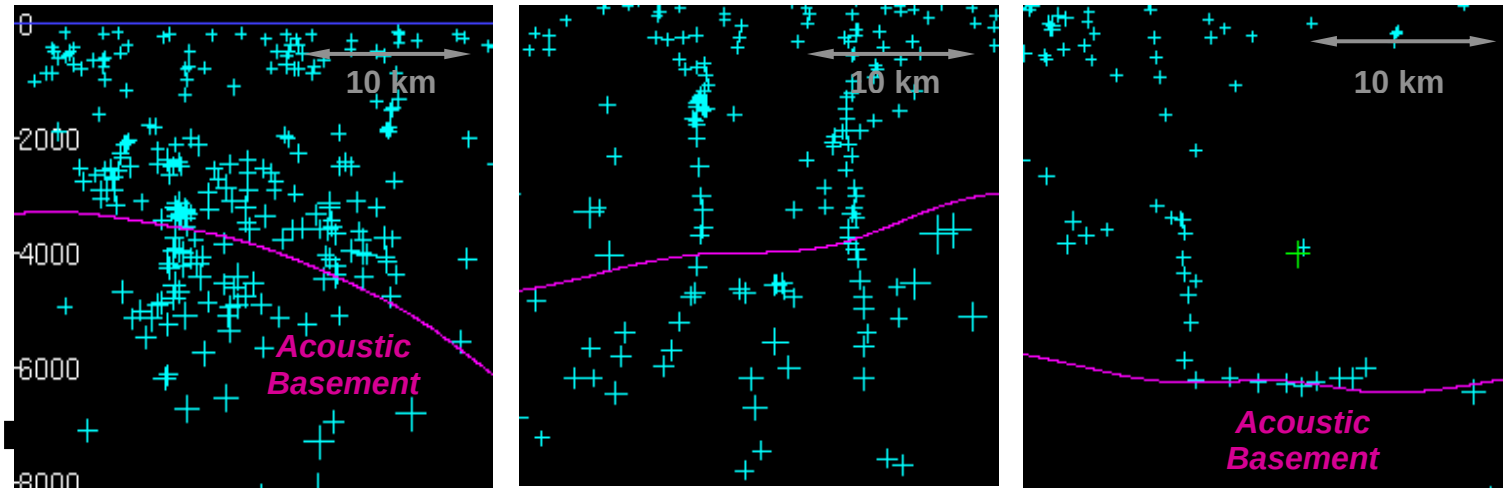
0
2000
4000
6000
10 km
Acoustic
Basement
10 km
10 km
Acoustic
Basement

Figure 4.

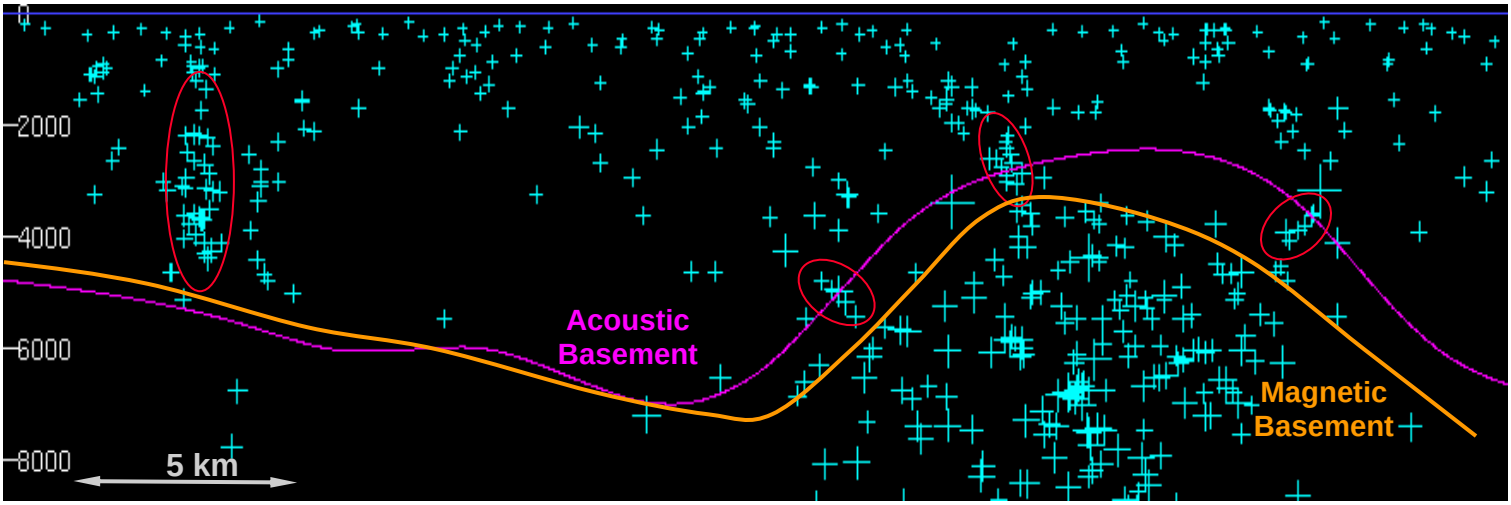
0
2000
4000
6000
8000
5 km
Acoustic
Basement
Magnetic
Basement

Figure 5.

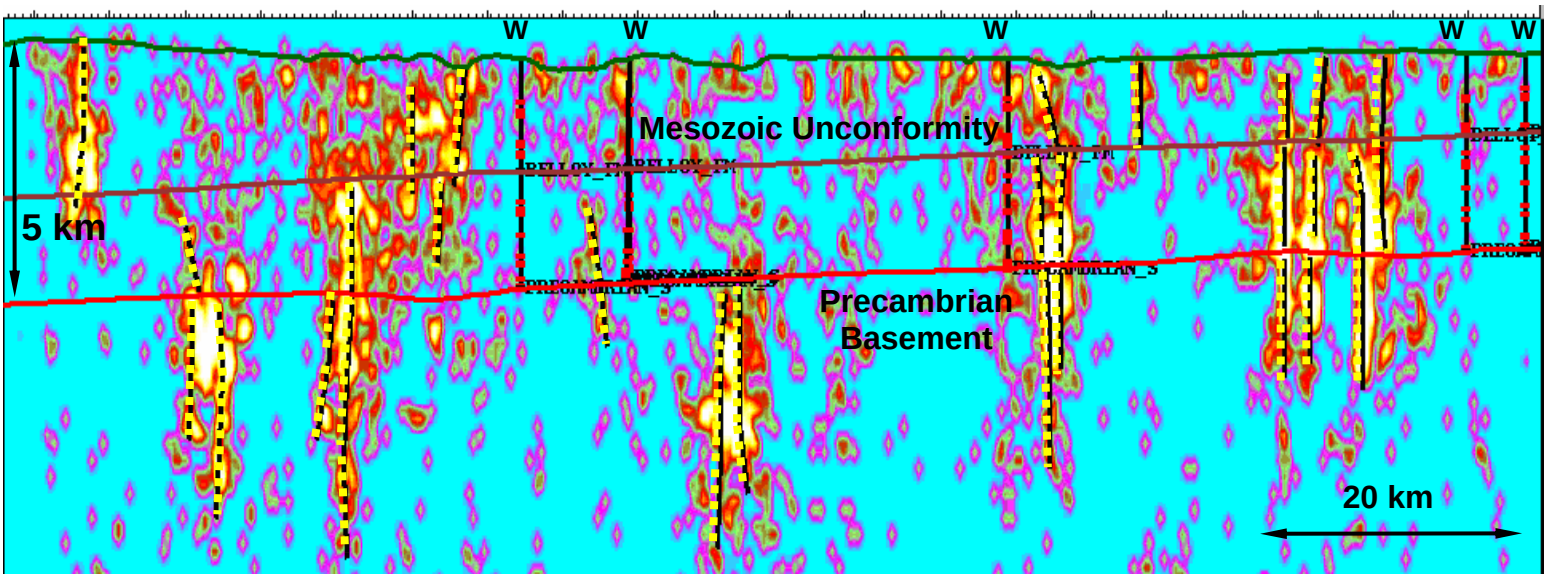
W
W
W
W
W
Mesozoic Unconformity
5 km
Precambrian
Basement
20 km

Figure 6.

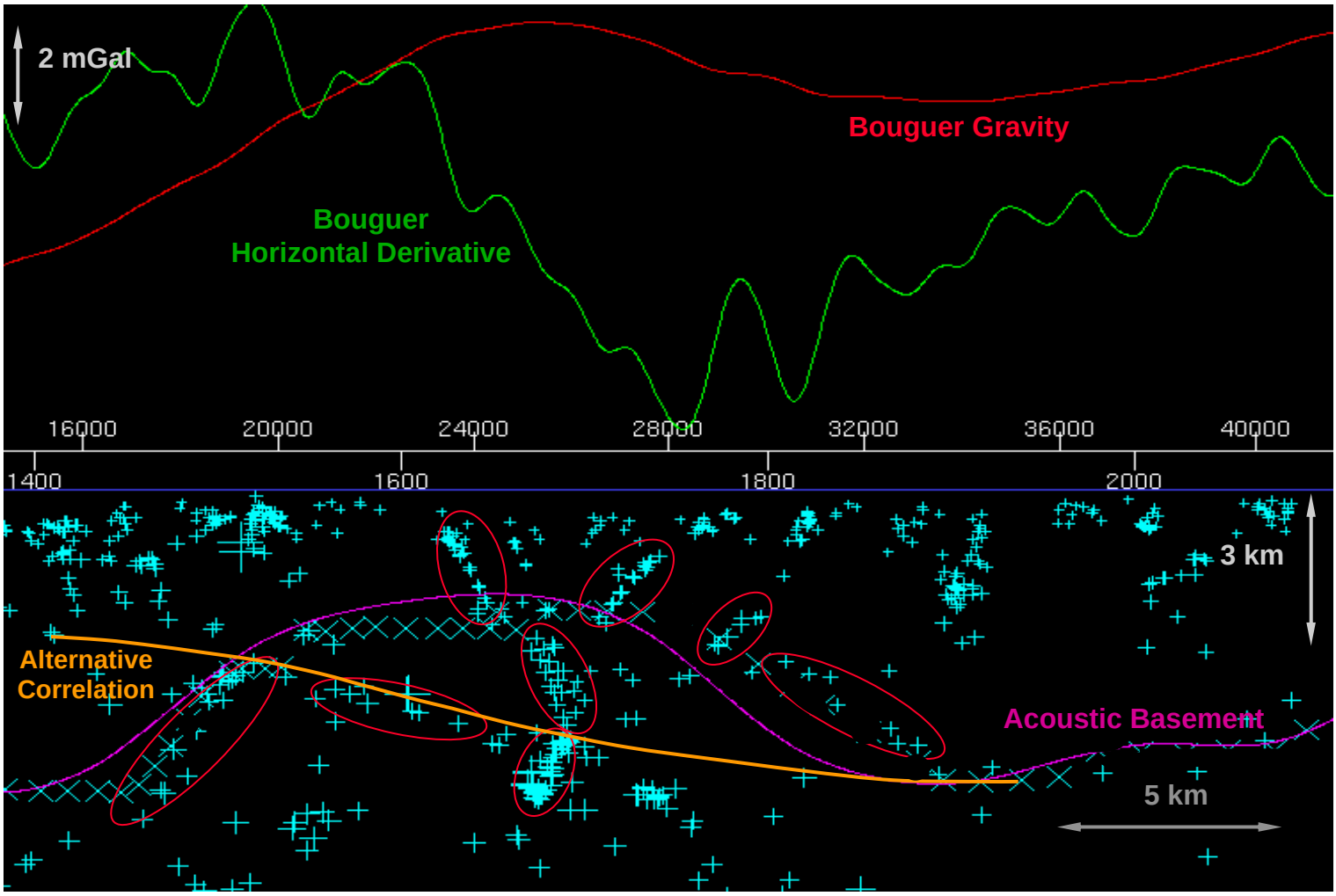
2 mGal
Bouguer Gravity
Bouguer
Horizontal Derivative
16000
20000
24000
28000
32000
36000
40000
1400
1600
1800
2000
3 km
Alternative
Correlation
Acoustic Basement
5 km

Figure 7.

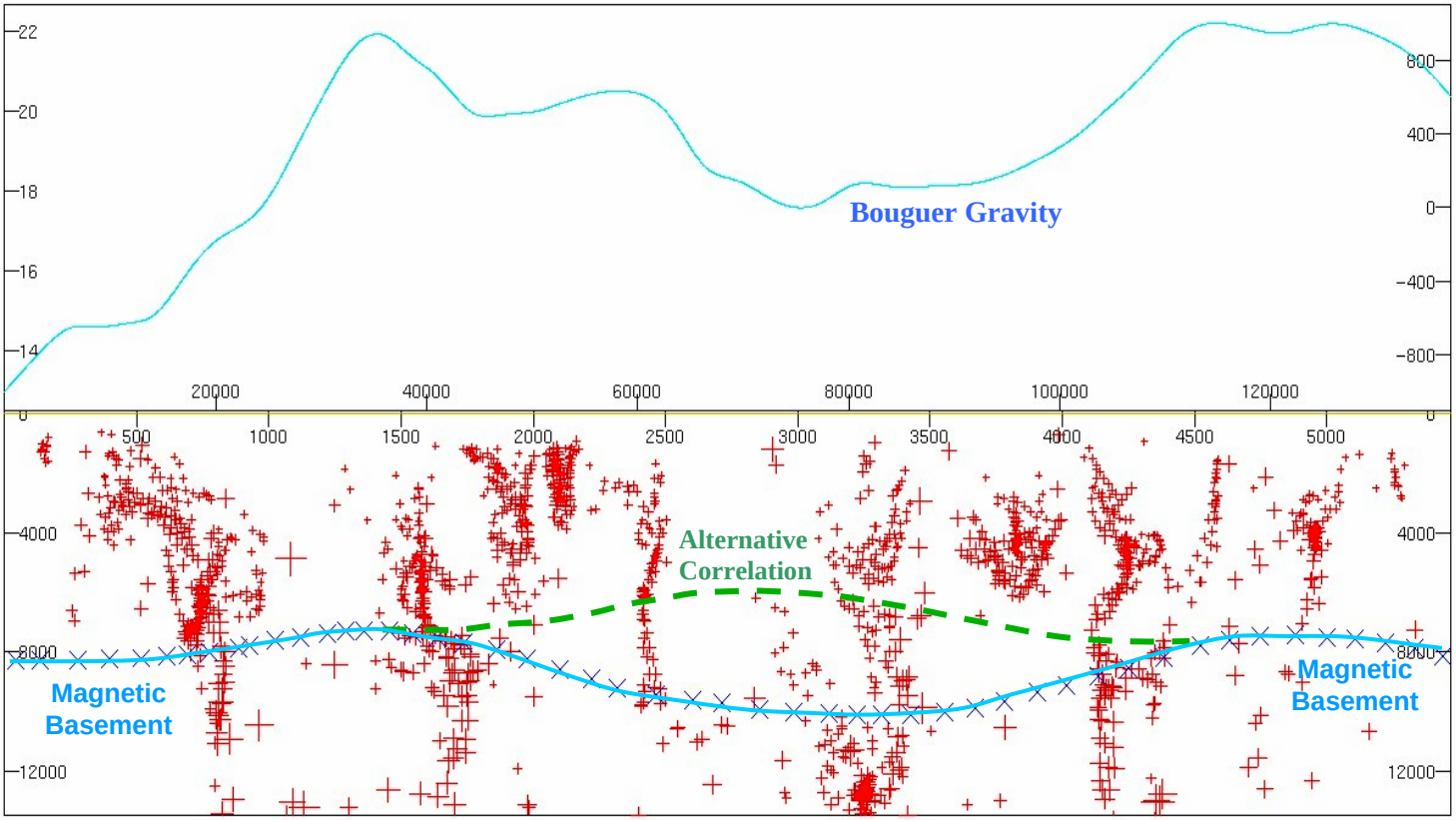
Bouguer Gravity
Alternative Correlation
Magnetic Basement
Magnetic Basement